JOURNAL OF THERMOPHYSICS AND HEAT TRANSFER
Vol. 19, No. 3, July–September 2005

Simulation of Electrical and Thermal Behavior of Conductive Polymer Composites Heating Elements

G. Droval,* P. Glouannec,† J. F. Feller,‡ and P. Salagnac§
South Brittany University, 56321 Lorient, France

Experimental and modeling studies were performed to describe the electrical and thermal behavior of two diphasic conductive polymer composites when subjected to electrical potential difference. The evolution of effective thermal conductivity of the conductive phase, poly(ethylene–co–ethyl acrylate)–carbon black or poly(amide12–b–tetramethyleneglycol)–carbon black, have been measured and compared to existing empirical models as a function of filler content. The diphasic materials were obtained by blending a conductive phase with an insulating polymer, poly(butylene terephthalate). The thermophysical characteristics of the diphasic materials were measured as a function of temperature. Ohmic heating experiments were performed on extruded tapes. A two-dimensional finite element model has been developed to determine the thermal and electrical behavior of these devices. The numerical and experimental results were in good agreement. This original use of diphasic material shows their interest in achieving heating elements.

Nomenclature

C_p	=	specific heat capacity, $J \cdot kg^{-1} \cdot K^{-1}$
E	=	electric field, $V \cdot m^{-1}$
h_c	=	convective heat coefficient, $W \cdot m^{-2} \cdot K^{-1}$
h_r	=	radiation heat coefficient, $W \cdot m^{-2} \cdot K^{-1}$
I	=	intensity, A
J	=	current density, $A \cdot m^{-2}$
k	=	thermal conductivity, $W \cdot m^{-1} \cdot K^{-1}$
Nu	=	Nusselt number
P	=	power, W
p	=	internal heat source, $W \cdot m^{-3}$
Ra	=	Rayleigh number
T	=	temperature, °C
T_c	=	center temperature, °C
T_s	=	surface temperature, °C
T_{air}	=	air temperature, °C
U	=	voltage, V
α	=	thermal diffusivity, $m^2 \cdot s^{-1}$
ρ	=	density, $kg \cdot m^{-3}$
σ	=	electrical conductivity, $S \cdot m^{-1}$
ϕ	=	volume fraction, %
φ	=	heat flux, $W \cdot m^{-2}$

Subscripts

c	=	composite
f	=	filler
m	=	matrix

Introduction

CONDUCTIVE polymer composites (CPC) resulting from the blending of an insulating polymer matrix with electrical conductive fillers (carbon black, carbon fibers, or metal particles) exhibit several interesting features due to their electrical conductivity variation with thermal solicitations.[1–5] This versatility of CPC is used for "intelligent" applications, such as self-regulated heating[6,7] or sensing. However, this important sensitivity of CPC to its environment also means that a good control of final properties is impossible if the numerous influent factors involved during the formulation and processing are not controlled.

One of the most significant factors is the filler distribution within the matrix, which results from processing conditions (temperature, shearing, viscosity, and orientation), formulation (filler content, molecular weight, and crystallinity of the polymer[2]), solubility parameters, particle/particle and particle/macromolecule interactions,[3,4] and spatial parameters as shape factor of the conducting particles[8] or exclusion domains into which particles cannot go.[3–5,9] For many applications, to obtain low-cost CPC and make the processing easier, it is helpful to decrease the percolation threshold, that is, the filler content over which the CPC becomes conductive. This can be achieved using cocontinuous multiphasic CPC[3,5] in which the filler is dispersed in only one continuous polymer phase.

Despite the numerous advantages of multiphasic CPC, their low thermal conductivity resulting from their high insulating polymer content is a drawback in achieving high thermal efficiency and allowing good heat dissipation. In fact, the current crossing through the filled polymer induces internal power generation by a joule effect, leading to a high thermal gradient between the center and surface of the material. One possible solution to overcome this problem is to improve thermal conductivity by introducing a thermally conductive filler into the matrix. However, this addition of filler will also have consequences on the electrical conductivity of the CPC. In view of this, the objective of this study is to quantify the effect of filler content and to understand the different phenomena involved during ohmic heating with CPC.

In the first part, we present some thermal conductivity models of dispersed particles in continuous phase. In the second part, we compare the evolution of effective thermal conductivity of poly(ethylene–co–ethyl acrylate)–carbon black (EEA–CB) and poly(amide12–b–tetramethyleneglycol)–carbon black (PEBAX–CB) with existing models for dispersed particles. Then the preceding CPC (EEA–CB and PEBAX–CB) were blended with poly(butylene terephthalate) (PBT), and we study the thermophysical characteristics of these diphasic CPC, which are rather different in composition and structure. In the last part, we investigate the electrical and thermal coupling phenomena on the characterized materials. Ohmic heating experiments were performed on extruded tapes.

Received 9 August 2004; revision received 10 November 2004; accepted for publication 11 November 2004. Copyright © 2005 by the American Institute of Aeronautics and Astronautics, Inc. All rights reserved. Copies of this paper may be made for personal or internal use, on condition that the copier pay the $10.00 per-copy fee to the Copyright Clearance Center, Inc., 222 Rosewood Drive, Danvers, MA 01923; include the code 0887-8722/05 $10.00 in correspondence with the CCC.

*Graduate Research Student, Laboratory of Thermal Studies, Energetic and Environment, Research Center, B.P. 92116.

†Professor, Laboratory of Thermal Studies, Energetic and Environment, Research Center, B.P. 92116.

‡Professor, Laboratory of Polymer Properties at Interfaces and Composites, Research Center, B.P. 92116.

§Lecturer, Laboratory of Thermal Studies, Energetic and Environment, Research Center, B.P. 92116.

Thermal Conductivity Models

Conductivity of Monophasic CPC

Several empirical models predicting the effective thermal conductivity k_c of a composite as a function of the filler volume content ϕ for known thermal conductivities k_m and k_f of the matrix and the filler, respectively, may be found in the literature.[10–13] As underlined in Ref. 14, effective heat transfer by conduction requires not only high thermal conductivity materials, but also good thermal contact between filler and matrix. The shape and size of particles (spheres, cubes, or fibers) were also found to influence effective heat transfer.[10]

The effective thermal conductivity k_c for low values of volume fraction for randomly distributed and noninteracting homogeneous spheres in a homogeneous medium is given by Maxwell's model[15] (also see Ref. 10),

$$k_c = k_m \frac{k_f + 2k_m + 2\phi(k_f - k_m)}{k_f + 2k_m - \phi(k_f - k_m)} \tag{1}$$

Some additional experimental considerations were introduced in the Lewis[16] and Nielsen[17] model[10] through nonadjustable parameters related to particle geometry and maximum packing volume fraction ϕ_m of these particles as described by

$$k_c = k_m \frac{1 + A\beta\phi}{1 - \beta\phi\left\{1 + \left[(1 - \phi_m)/\phi_m^2\right]\phi\right\}} \tag{2}$$

with

$$\beta = \frac{(k_f/k_m) - 1}{(k_f/k_m) + A}$$

where the constant A depends on the dispersed particles shape and orientation. Here ϕ_m is the maximum packing volume fraction of the dispersed particles. The values of A and ϕ_m for many geometric shapes and orientation are available in the literature[10] and are given in Tables 1 and 2 for spherical particles and aggregates of spheres. This model describes fairly well effective thermal conductivity when the thermal conductivity of the continuous phase is much smaller than that of the dispersed phase, which is the case with our systems.

The Agari and Uno model [Eq. (3)] has been successfully applied for filled polymers (see Refs. 18 and 19),

$$k_c = k_f^{\phi C_2} C_1 k_m^{(1-\phi)} \tag{3}$$

C_1 and C_2 are constants determined experimentally, which must be positive and lower or equal to the unity. C_1 represents the effect of particles on crystallinity or the crystal size of the polymer. C_2 becomes closer to one when the particles can easily form conductive chains through the material.

Table 1 Values of A for spheres

Type of dispersed phase	Direction of heat flow	A
Spheres	Any	1.50
Aggregates of spheres	Any	$(2.50/\phi_\alpha)^a - 1$

[a]Maximum packing volume fraction of the spheres in the aggregates.

Table 2 Values of ϕ_m for spheres

Shape of particle	Type of packing	ϕ_m[a]
Spheres	Face-centered cubic	0.7405
Spheres	Body-centered cubic	0.60
Spheres	Simple cubic	0.524
Spheres	Random	0.637

[a]Maximum packing volume fraction of the spheres in the matrix.

Conductivity of Diphasic CPC

For a two-phase system structured in layers, thermal conductivity is the lowest when the conductive layers are arranged perpendicular to the heat flow direction and can be well described by the harmonic mean model[10] expressed in Eq. (4), whereas when the thermal flow direction is parallel to the layers the thermal conductivity is the highest and is determined by the arithmetic mean model[10] expressed in Eq. (5).

Harmonic mean model:

$$k_c^{-1} = k_f^{-1}\phi + k_m^{-1}(1 - \phi) \tag{4}$$

Arithmetic mean model:

$$k_c = k_f\phi + k_m(1 - \phi) \tag{5}$$

When the phases are randomly distributed, the geometric mean model[10] applies according to

$$k_c = k_f^{\phi} k_m^{(1-\phi)} \tag{6}$$

CPC Characterization

In a first step, the influence of carbon black particles on the thermal conductivity of monophasic CPC with two polymer matrices (EEA and PEBAX) was investigated. The evolution of effective thermal conductivity as a function of filler content was measured and compared to empirical models such as those of Maxwell,[5] Lewis,[16] Nielsen,[17] and Agari et al.[18,19]

In a second step, thermophysical properties were measured as a function of temperature for two diphasic thermoplastic CPC. These two materials were obtained by blending in the melt the conductive phase (EEA–CB or PEBAX–CB) with PBT. The blends are assumed to be isotropic at macroscopic scale due to the relatively small size of CB aggregates, 200–600 nm, with regard to the samples size used.

Material

The desired conducting phase composition was adjusted by blending EEA-37% w/w CB or PEBAX-40% w/w CB master batches with pure EEA or PEBAX, respectively. For instance, EEA-27.75% CB was obtained by blending pure EEA with 75% of a master batch containing 37% w/w of CB. The so-called conducting phase is constituted of EEA or PEBAX (thermoplastic copolymers) in which electrically conducting particles of CB are dispersed, whereas PBT provides the diphasic CPC with mechanical and thermal stability, even if the conductive phase reaches the liquid state. The main polymer characteristics may be found in Table 3 with T_m and T_g the melting and glass transition temperature, respectively.

Depending on the sample thickness required for each characterization technique, the blending process chosen was either a Brabender Laboratory station internal mixer to obtain 10-mm-thick molded pads pressed up to 5×10^6 Pa, or a Brabender Laboratory station twin screw extruder to obtain 3-mm-thick tapes.

Experimental Measurements

The effective thermal conductivity was measured with a precision of 10% by a guarded hot plate method at a temperature of less than 75°C. The samples were 10-mm-thick pads of a 60×60 mm^2 section.

Thermal diffusivity α was determined by the laser flash method. The Nd/glass pulse laser of 1.06-μm wavelength has an energy pulse up to 8 J with a pulse duration of 0.4 ms. The thermal diffusivity of

Table 3 Polymer composites characteristics

Property	EEA	PEBAX	PBT
T_m, °C ± 0.5	99.5	165	226
T_g, °C ± 2	−33 ± 3	−41 ± 1	42 ± 3
Density at 27°C, kg · m^{-3}	930	1010	1310
k, W · m^{-1} · K^{-1}	0.25	0.24	0.23

the sample was calculated from the temperature vs time curve using the Parker method through an iterative procedure (see Ref. 20). The samples were disks 20 mm in diameter and 2 mm thick. The precision of these measurements is within 5%.

Specific heat capacity C_p was measured using a differential scanning calorimeter (DSC) (Mettler Toledo Model 822^e) with a disk-type measuring system. A three-curve analysis method was used. This involved obtaining DSC sapphire (22.1 mg) sample, baseline, and reference material. Sample weights were chosen to be close to the sapphire and were approximately 15 mg. The measurements were taken at $15°C \cdot min^{-1}$ under dry nitrogen flow to prevent oxidative degradation and pollution of the samples. In this case, the precision of specific heat measurements is within 3%.

Density measurements were made with a pycnometer at room temperature (27°C) in methanol. To determine the density variation as a function of temperature, the thermal expansion coefficient of the CPC was measured by a dynamic mechanical analyzer (TA Instruments, Model 2980) with a static force of 0.01 N in the compression mode and a temperature sweep of $3°C \cdot min^{-1}$. The samples were disks 13 mm in diameter and 3 mm thick. This process leads to a precision within 2%.

Thermal Conductivity of CPC Conducting Phase

The thermal conductivity of most polymers is close to $0.25\ W \cdot m^{-1} \cdot K^{-1}$ and for CB it ranged from 6 to $175\ W \cdot m^{-1} \cdot K^{-1}$, depending on its state.[8] To predict the effective thermal conductivity, an intermediate value of k_f can be used for dispersed particles models without significant error.[12] As shown in Fig. 1, for a constant filler volume content of 20%, the two models, Maxwell[15] and Lewis[16] and Nielsen,[17] have an asymptotic evolution. This means that for sufficiently high values of $k_f/k_m (>20)$, the effective thermal conductivity of the composite is only a function of filler content.

The evolution of the effective thermal conductivity of EEA–CB and PEBAX–CB compared to dispersed particles models is shown in Figs. 2 and 3, respectively. It can be seen from Figs. 2 and 3 that k_c can only be increased by a factor of two over 25% of fillers, which unexpectedly also lead to an important modification of rheological properties of CPC.

For EEA–CB (Fig. 2), a very good fit with experimental data was obtained with use of the Maxwell and Lewis and Nielsen models ($A = 1.5$ and $\phi_m = 0.637$). These two models are superimposed because they correspond to a random distribution of spherical particles (Tables 1 and 2). The coefficients derived from fitting the data in the Agari et al. model, $C_1 = 1$ and $C_2 = 0.5$, also suggest that CB, dispersed in the amorphous phase, may have an impact on EEA crystallinity, as already noticed previously by DSC experiments in another work.[20] On the other hand, randomly packed aggregates of spheres, corresponding to the Lewis and Nielsen model ($A = 3$ and $\phi_m = 0.637$), do not seem suitable for this material. In fact, in EEA–CB, which is a statistical copolymer, CB is better dispersed in the matrix due to strong CB particles/polymer chain interactions[21]

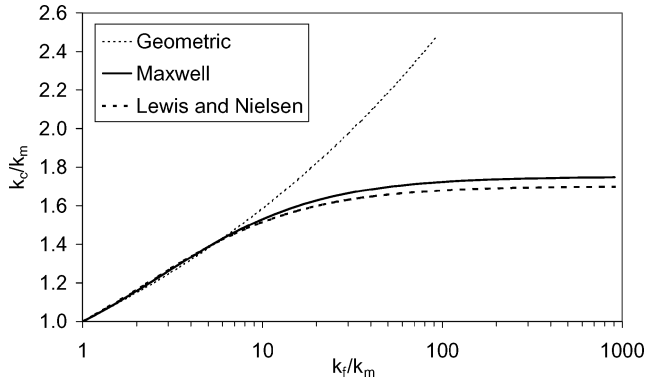

Fig. 1 Comparison of models predicting effective thermal conductivity of composite materials, for constant filler content of 20% by volume and $1 \le k_f/k_m \le 1000$.

Table 4 Diphasic CPC composition

	Composition, % w/w		
N°CPC	PBT	EEA-27.7%CB[a]	PEBAX-12%CB[b]
1	60	40	——
2	60	——	40

[a]Volume fraction $\phi_{CB} = 16.5\%$. [b]Volume fraction $\phi_{CB} = 7.6\%$.

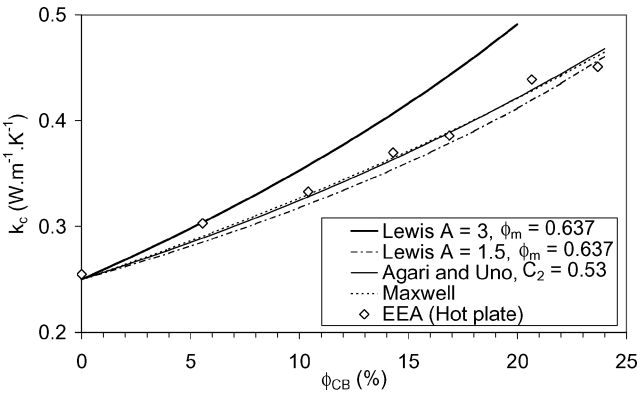

Fig. 2 EEA–CB, effective thermal conductivity as a function of volume fraction of CB at 50°C.

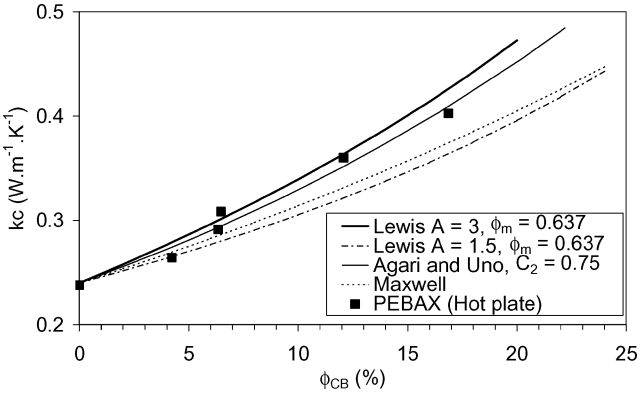

Fig. 3 PEBAX–CB, effective thermal conductivity as a function of volume fraction of CB at 50°C.

and to its random structure. Because it is not realistic to establish that each elementary spherical particle of CB (diameter between 20 and 40 nm) could be found alone in the polymer matrix, it must be deduced from these models that the correct observation scale is that of CB particle aggregates (size between 200 and 800 nm), which consequently should have a spherical shape.

For PEBAX–CB (Fig. 3), the Lewis and Nielsen model ($A = 3$ and $\phi_m = 0.637$), corresponding to randomly packed aggregates of spheres, seems more suitable for this material. Therefore, these aggregates of spheres are more sizable than that of EEA–CB. A fit with the Agari et al. model leads to a same value of C_1 and a higher value of C_2 coefficient in comparison to EEA–CB, which is reasonable because this copolymer leads to a microphase separation due to its block nature, and this may result in a more heterogeneous dispersion of carbon black aggregates during processing.

However, there is a tendency for the random distribution of particles or aggregates of CB because both EEA and PEBAX are semicrystalline polymers. Also, it is well known that CB aggregates are too large to be incorporated in crystalline lamellas.

Thermophysical Properties of Diphasic CPC

Diphasic CPC were processed blending 40% w/w of the conducting phase EEA–27.75%CB or PEBAX–12%CB (earlier formulated at 180°C) with 60% w/w of PBT (at 250°C), in a Fairex single screw extruder. The diphasic CPC composition (Table 4) chosen was

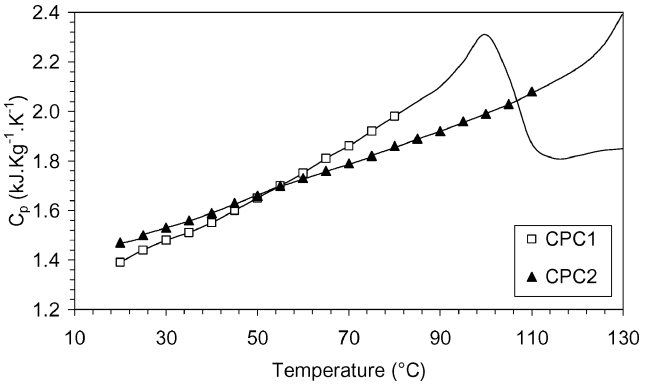

Fig. 4 CPC_1 and CPC_2 specific heat capacity evolution with temperature.

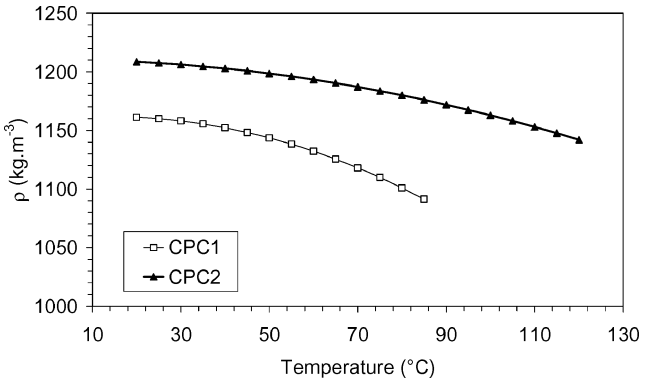

Fig. 5 Density evolution with temperature for CPC_1 and CPC_2.

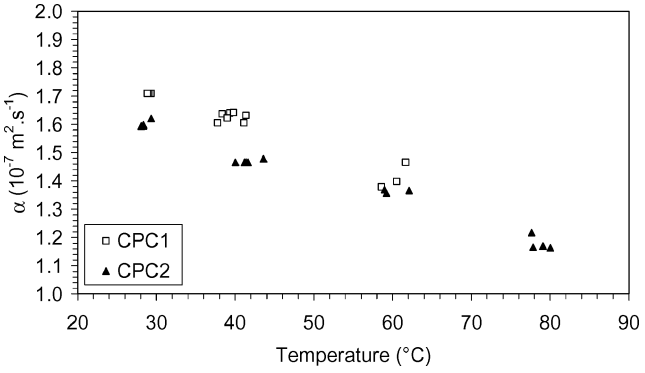

Fig. 6 Thermal diffusivity evolution of CPC_1 and CPC_2 with temperature.

determined with regard to electrical properties (resistivity and percolation threshold) and morphological considerations (cocontinuity).[5]

Figure 4 shows the equivalent specific heat capacity C_p curve obtained by DSC. The curve obtained for CPC_1 shows that some of EEA crystals began to melt at over 80°C, which is why C_p was only evaluated in the temperature range considered (20–80°C). For PEBAX, in which crystals melt over, the specific heat C_p was determined in the temperature range 20–110°C.

Figure 5 shows that CPC_2 has a slightly higher density than CPC_1 despite of its lower CB content, the large scale used emphasizes this difference. This agrees with classical mixing law, when a CB density of 1 750 $\mathrm{kg \cdot m^{-3}}$ and values of polymers density given in Table 3 are used.

Thermal diffusivities α of CPC_1 and CPC_2 measured by laser flash technique are given in Fig. 6. Because the temperature at the front surface, which is exposed to the laser flash, increases some degrees above the oven temperature, the experimental temperature range was restricted to 20–60°C for CPC_1 and to 20–80°C for CPC_2. In these

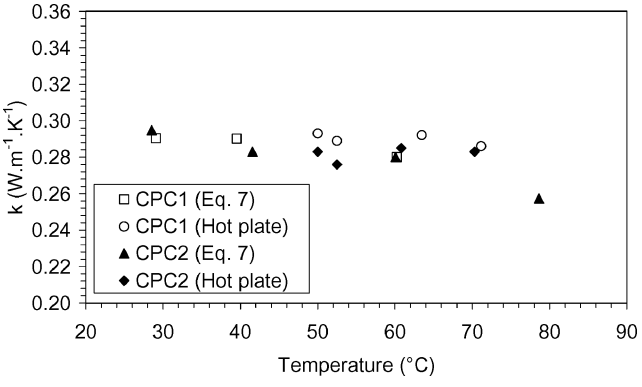

Fig. 7 Thermal conductivity of CPC_1 and CPC_2 with temperature.

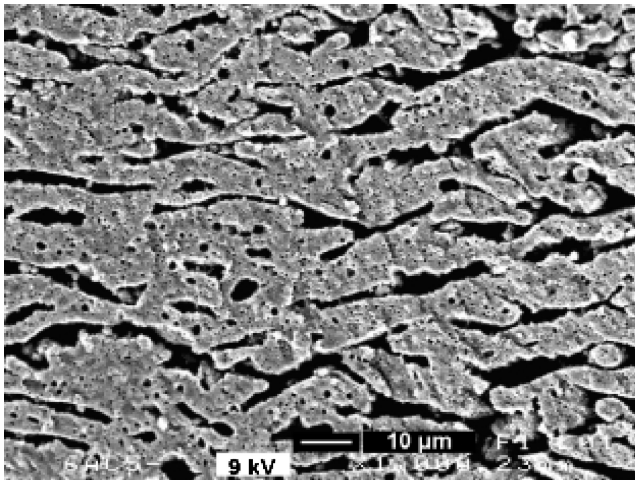

Fig. 8 CPC_1 morphology observed by SEM.

temperature ranges, the thermal diffusivity evolution is assumed to be linear, which agrees with the literature.[20] Thermal conductivity can be deduced from the three parameters α, ρ, and C_p using

$$k = \alpha \rho C_p \tag{7}$$

The experimental results obtained by the guarded hot plate method (Fig. 7) compared to those calculated with Eq. (7) are found to be in good agreement.

Classical mixing laws can be used to predict the effective thermal conductivity of the diphasic CPC, when both PBT and EEA–27.75%CB or PEBAX–12%CB are considered as two homogeneous phases called the matrix and the electrically conducting phase, respectively. This assumption is reasonable because EEA–CB and PEBAX–CB are both immiscible with PBT; the resulting diphasic CPC has a cocontinuous morphology, as can be seen in Fig. 8. Different morphologies can be observed in such diphasic CPC with regards to the considered scale. Morphologies were observed with a scanning electron microscope (SEM) (JEOL) after fracture of the samples in liquid nitrogen. In the conducting phase (here solvent extracted for observation) CB aggregates of several hundreds of nanometers are dispersed and associated to form conductive pathways through the polymer matrix. When the whole sample is considered at a larger scale, the conducting phase forms channels or lamellas of several micrometers thick in the extrusion direction. This is equivalent to the arithmetic or harmonic mean model.

A comparison of the results from harmonic, geometric, and arithmetic models are given in Table 5. All of the calculated values from the models considered are in rather good agreement with experimental data. This is because all of the models give similar values for a ratio $k_f/k_m \leq 2$, which is the case here with $k_{\mathrm{PBT}} = 0.23\ \mathrm{W \cdot m^{-1} \cdot K^{-1}}$, $k_{\mathrm{EEA27.75\%CB}} = 0.4\ \mathrm{W \cdot m^{-1} \cdot K^{-1}}$, and $k_{\mathrm{PEBAX12\%CB}} = 0.3\ \mathrm{W \cdot m^{-1} \cdot K^{-1}}$.

Table 5 Comparison between theoretical thermal conductivity and measured values of CPC at 50°C

Model	CPC_1[a]	CPC_2[b]
Measured	0.29	0.28
Harmonic	0.28	0.26
Arithmetic	0.31	0.27
Geometric	0.29	0.26

[a]Where $k_{EEA27.75} = 0.4\ W \cdot m^{-1} \cdot K^{-1}$. [b]Where $k_{PEBAX12} = 0.3\ W \cdot m^{-1} \cdot K^{-1}$.

Table 6 Tapes dimension

CPC	Length, mm	Width, mm	Thickness, mm
1	185	38	3.55
2	180	50	5.0

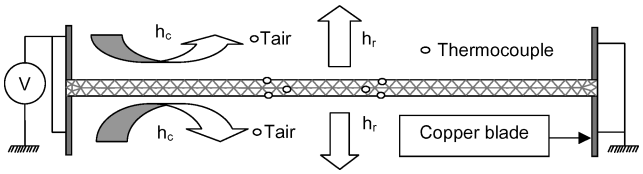

Fig. 9 Longitudinal cross section of an extruded tape, from the top.

Electrical and Thermal Responses of Two CPC

To study the electrical and thermal coupling behavior in the diphasic materials characterized earlier, experimental work has been carried out on extruded tapes subjected to direct current, as is the case during ohmic heating. The thermophysical data determined earlier together with these additional experiments allowed the development of a two-dimensional numerical model to simulate the thermoelectrical behavior.

Experimental Device

The samples were extruded tapes of small thickness (Table 6) placed horizontally on edge (Fig. 9) and connected to current by two copper electrodes at each end. To improve the electrical contact, the ends were painted with silver paint. In this study, the heat transfers at the surface were free convection and radiation.

The temperatures at the center of the material and at the surface were measured by type K thermocouples, 250 μm in diameter. The ambient air, T_{air}, was also measured on each side (Fig. 9). The temperature, voltage, and intensity were measured with respect to time by the data acquisition system. Experimental uncertainties were attributed to the measurement of temperature (± 1.0°C), voltage (± 0.5 V), intensity (± 2 mA), and implementation of thermocouples in situ (± 50 μm).

Mathematical Modeling

Mathematical modeling was developed with FEMLAB® to predict the thermal and electrical responses of the extruded tapes. FEMLAB uses the finite element method.[22,23] The materials were taken to be isotropic and homogenous at the macroscopic scale. The governing equation for the electrical conduction in the material is the Laplace equation (see Ref. 23),

$$-\nabla \cdot [\sigma(T)\nabla V] = 0 \tag{8}$$

where ∇ denotes the gradient, $\nabla\cdot$ the divergence, and $\sigma(T)$ the electrical conductivity function of temperature.

The heat transfer is governed by the heat equation,

$$\rho C_p \frac{\partial T}{\partial t} = \nabla \cdot (k\nabla T) + p \tag{9}$$

where p is the internal power generated by electricity defined as

$$p = \sigma E^2 \tag{10}$$

Figure 9, which is a longitudinal cross section of the extruded tape, describes the geometry and mesh. The voltage is applied to each end of the tape. The copper blades electrodes are not taken into account because a perfect electrical contact is assumed. The thermal flow through the thickness can be neglected given the small thickness of the sample. The thermal boundary conditions applied to the vertical surfaces are only natural convection and radiation. During the experiment, the airflow is in a laminar condition, and so the convective coefficient h_c is given by a correlation used for a vertical plate,[24]

$$Nu = 0.59 Ra^{\frac{1}{4}} \tag{11}$$

where the Rayleigh number is between 10^4 and 10^9.

The radiation coefficient h_r is linearized[24] and given by

$$h_r = 4\varepsilon\sigma_s T^3 \tag{12}$$

with ε the emissivity of the tapes ($\varepsilon = 0.95$), σ_s the Stefan–Boltzman constant, and T the mean temperature in degrees Kelvin. (The surrounding environment is considered to be a blackbody.)

Different grids were tested. The mesh chosen was compromise between accuracy and time cost. The geometry was discretized with an unstructured grid of 288 finite triangular elements. A quadratic interpolation was used. For temporal discretization, an implicit formulation was applied. The coupled nonlinear partial differential equations (8) and (9) of the electric field and the thermal field with the boundary conditions were solved simultaneously with an absolute convergence temperature of 10^{-4} K.

Experimental Result

During the experiments, the voltage is increased by steps of 10 or 20 V and is then decreased before the temperature at the center, T_c, reaches the melting temperature T_m (Table 3) of the conducting phase.[25]

An example of measurements carried out on CPC_1 is given in Fig. 10. The intensity curve emphasizes the self-regulation phenomenon, which begins close to 60°C. During a voltage step, the intensity instantaneously increases before it progressively decreases and reaches steady state. This phenomenon is reversed during cooling. The self-regulation phenomenon is due to the variation of the electrical conductivity with temperature determined by voltage and intensity measurements (Fig. 11). Figure 11 shows that the two CPC have very different electrical characteristics despite their rather similar thermal behavior. At room temperature, the electrical conductivity of CPC_1 is roughly twice that of the CPC_2. Moreover, the electrical conductivity drops with heating. This effect, called positive temperature coefficient, starts about 25°C for CPC_1 and about 80°C for CPC_2.

Simulated Result

Comparison of experimental measurements with simulated data is done by direct reading of the voltage and air temperature variation values in the experimental file. Thermophysical properties are

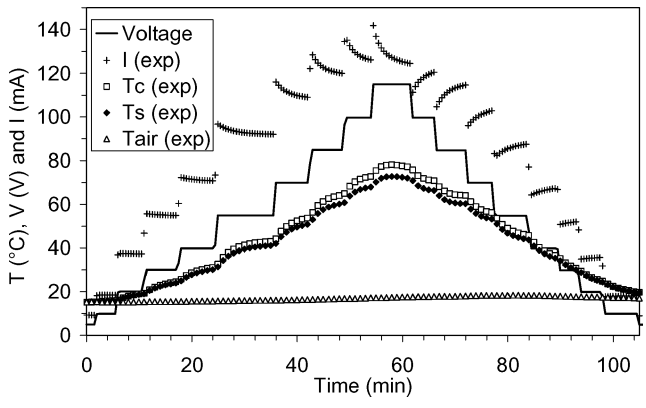

Fig. 10 Experiment performed with CPC_1 extruded tape.

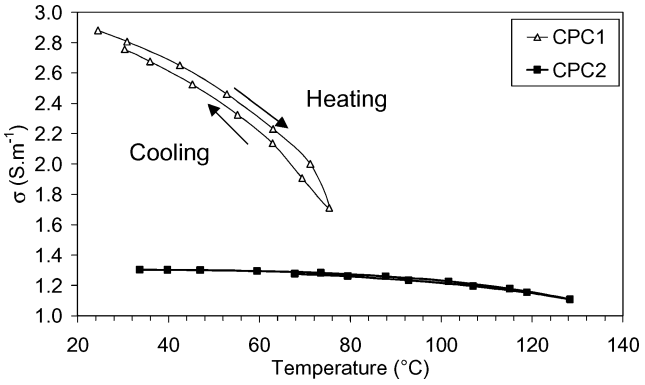

Fig. 11 Electrical conductivity of CPC_1 and CPC_2 as a function of temperature.

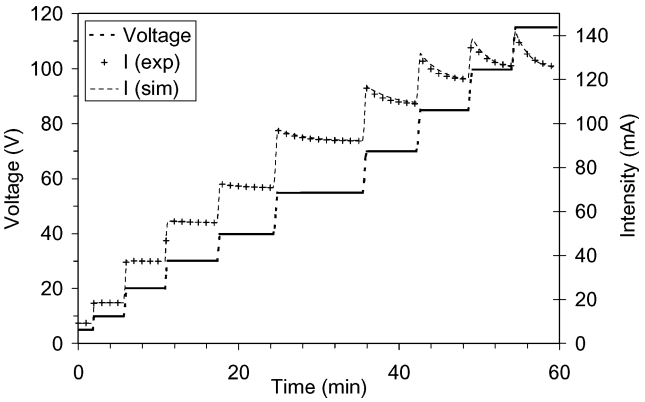

Fig. 12 Simulation of CPC_1 intensity response compared to experimental values.

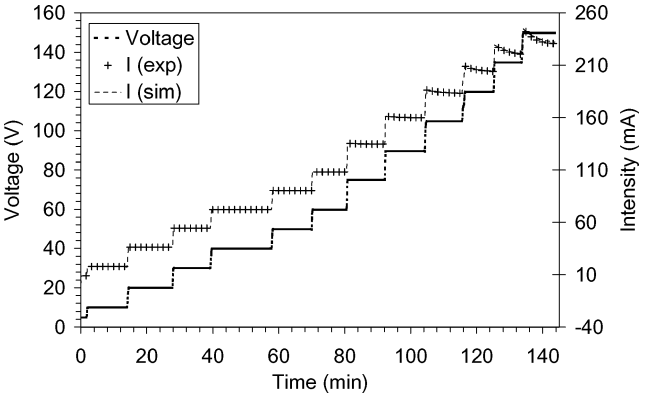

Fig. 13 Simulation of CPC_2 intensity response compared to experimental values.

brought into the model through polynomial equations. In this study, only heating data were considered. The experimental temperature corresponds to the average values measured at the center and surface of the tapes. The simulated intensity (Figs. 12 and 13) and temperature (Figs. 14 and 15) responses are in good agreement with experimental data for both CPC. The electrical intensity was calculated from the current density J at the middle section of the tape.

Figures 16 and 17 give additional information on the heating behavior of the CPC: It appears that, due to the presence of a thermal gradient between the two main surfaces of the sample, the current density J is not constant in the thickness of the material. Figures 16 and 17, obtained in quasi-stationary-state conditions for different voltage levels, show that the electrical power tends to be generated at the surfaces where the temperature is lower and, thus, the electrical conductivity higher. Table 7 lists measured temperatures and the heat flux. When it is assumed that steady state is reached, all of the

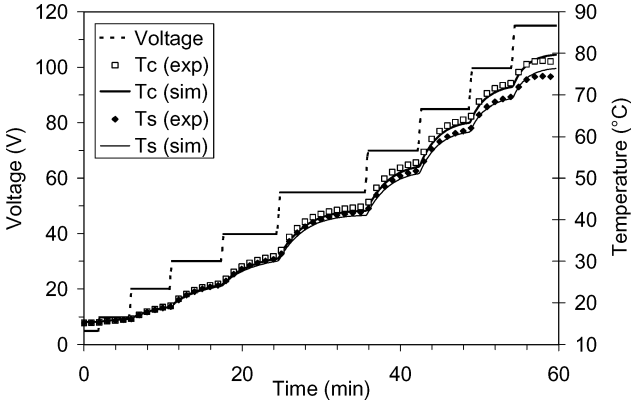

Fig. 14 Simulation of CPC_1 temperature response compared to experimental values.

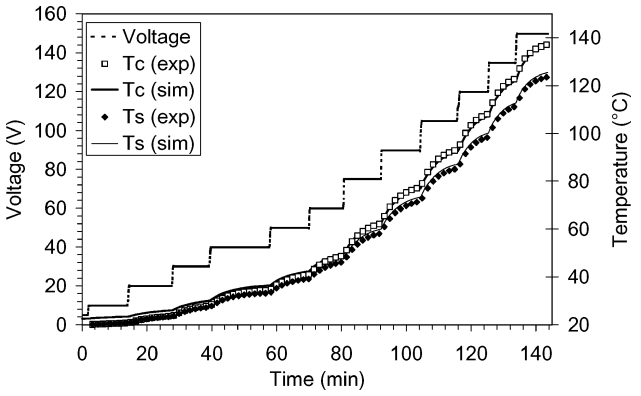

Fig. 15 Simulation of CPC_2 temperature response compared to experimental values.

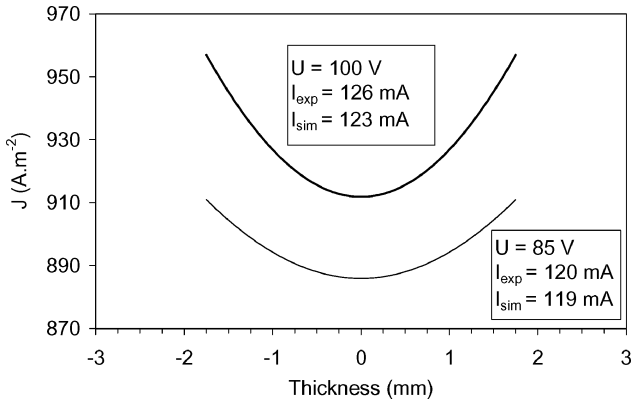

Fig. 16 Simulation of the current density profile for CPC_1 at two voltages.

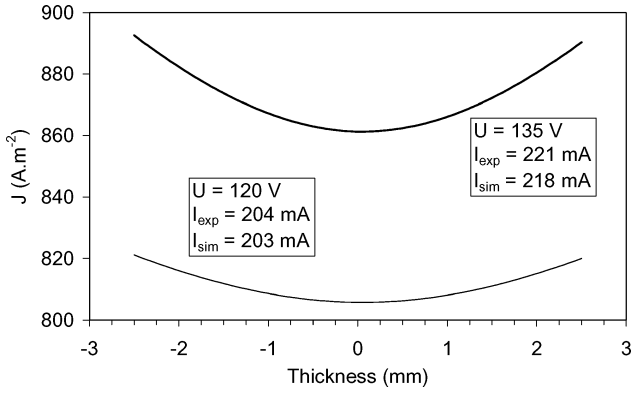

Fig. 17 Simulation of the current density profile for CPC_2 at two voltages.

Table 7 Results in quasi-stationary regime for two voltage solicitations

U, V	P, W	$T_{c\,(\mathrm{exp})}$, °C	$T_{s\,(\mathrm{exp})}$, °C	$\varphi_{(\mathrm{exp})}$, kW · m^{-2}	$h_{g\,(\mathrm{exp})}$, W · m^{-2} · K^{-1}	$h_{c\,(\mathrm{sim})}$, W · m^{-2} · K^{-1}	$h_{r\,(\mathrm{sim})}$, W · m^{-2} · K^{-1}
				CPC$_1$			
85	10.2	64.3	60.4	0.8	16.7	8.5	6.5
100	12.6	72.9	68.0	0.9	17.6	8.9	6.8
				CPC$_2$			
120	24.4	108.2	98.4	1.3	17.3	9.2	7.8
135	29.7	123.0	111.3	1.7	19.0	9.4	8.3

electrical power is dissipated in the surroundings; thus, the heat flux can be expressed by

$$\varphi = P/S_e = h_g(T_s - T_{\mathrm{air}}) \tag{13}$$

where S_e is the vertical exchange surface and h_g the global exchange coefficient for both convection and radiation.

Therefore, the reason for the important temperature gradient evidenced in the sample thickness is that the CPC thermal conductivity is too low. For CPC_2, the temperature difference between the center and surface (only a 2.5-mm space) can reach 12°C for a heat flux of 1.7 kW · m^{-2}.

Moreover, to validate the boundary conditions used in the model, experimental exchange coefficient h_g values derived from measurements [Eq. (13)] have been compared to calculated values of convective h_c and radiation h_r coefficients. The results confirm the validity of the hypothesis chosen for the modeling. (Thermal exchange both through electrical connections and through the ends are negligible.) The difference between the global exchange coefficient h_g and the sum of convective h_c and radiation h_r coefficients is less than 10%.

Conclusions

The electrical and thermal properties of two diphasic CPC used for self-regulated heating have been investigated. In the first step, we have selected empirical models able to predict the thermal conductivity of the electrically conductive phase resulting from the dispersion of nanoparticles of conductive CB in an insulating polymer matrix. It appears that both the Lewis and Nielsen and the Agari et al. models are suitable for predicting the thermal conductivity evolution of the monophasic composite with filler content. To predict the thermal conductivity of the diphasic CPC, models based on classical mixing laws can be used. The best fit was obtained for PBT/EEA–CB, whereas for PBT/PEBAX–CB the points were more scattered, certainly due to microphase separations. Moreover, in the second step, the introduction of measured thermophysical data into a finite element method code allows the simulation of the thermoelectrical behavior of CPC with very good accuracy.

Additional results were demonstrated from the simulation as a surface-heating phenomenon, which showed that more power is generated at the surface, where the temperature is lower. The temperature gradient responsible for this is undesirable and may damage the material itself. To reduce this gradient, one solution may be to increase the thermal conductivity of the CPC. For this reason, we will now try to improve this characteristic. Our predictions show that incorporating up to 25% v/v of CB allows doubling of the CPC thermal conductivity, but has an important impact on rheological properties, which determines processing conditions and, thus, the CPC morphology. Also it must be taken into consideration that increasing the CB content will also increase electrical conductivity and, thus, the temperature gradient. Consequently, to solve this problem, a synergy between different fillers must be found.

References

[1] Narkis, M., and Tobolsky, A. V., "Chemically Crosslinked Polyethylene: Modulus–Temperature Relations and Heat Stability," *Journal of Applied Polymer Science*, Vol. 13, No. 11, 1969, pp. 2257–2263.

[2] Meyer, J., "Glass Transition Temperature as a Guide to Selection of Polymer Suitable for PTC Materials," *Polymer Engineering and Science*, Vol. 13, No. 5, 1973, pp. 462–468.

[3] Gubbels, F., Jérôme, R., Vanlathem, E., Deltour, R., Blacher, S., and Brouers, F., "Kinetic and Thermodynamic Control of the Selective Localization of Carbon Black at the Interface of Immiscible Polymer Blends," *Chemistry of Materials*, Vol. 10, No. 5, 1998, pp. 1227–1235.

[4] Zhang, C., Yi, X. S., Yui, H., Asai, S., and Sumita, M., "Morphology and Electrical Properties of Short Carbon Fiber-filled Polymer Blends: High-density Polyethylene/poly(methyl methacrylate)," *Journal of Applied Polymer Science*, Vol. 69, No. 9, 1998, pp. 1813–1819.

[5] Feller, J. F., Linossier, I., and Levesque, G., "Conductive Polymer Composites (CPC): Comparative Study of Poly(ethylene-co-ethyl acrylate)-carbon Black and Poly(butylene terephthalate)/poly(ethylene-co-ethyl acrylate)-carbon Black Electrical Properties," *Polymers for Advanced Technologies*, Vol. 13, No. 10-12, 2002, pp. 714–724.

[6] El-Tantawy, F., Kamada, K., and Ohnabe, H., "A Novel Way of Enhancing the Electrical and Thermal Stability of Conductive Epoxy Resin-carbon Black Composites via the Joule Heating Effect for Heating-element Applications," *Journal of Applied Polymer Science*, Vol. 87, No. 1, 2003, pp. 97–109.

[7] Ageorges, C., Ye, L., and Hou, M., "Experimental Investigation of the Resistance Welding for Thermoplastic-matrix Composites. Part I: Heating Element and Heat Transfer," *Composites Science and Technology*, Vol. 60, No. 7, 2000, pp. 1027–1039.

[8] Wolff, S., and Wang, M. J., *Carbon Black Science and Technology*, 2nd ed., Vol. 9, Marcel Dekker, New York, 1993, pp. 289–355.

[9] Feller, J. F., Bruzaud, S., and Grohens, Y., "Influence of Clay Nanofiller Incorporation on Electrical and Rheological Properties of Conductive Polymer Composite (CPC)," *Materials Letters*, Vol. 58, No. 5, 2004, pp. 739–745.

[10] Progelhof, R. C., Throne, J. L., and Ruetsch, R. R., "Methods for Predicting the Thermal Conductivity of Composite Systems: A Review," *Polymer Engineering and Science*, Vol. 16, No. 9, 1976, pp. 615–625.

[11] Kumlutaş, D., Tavman, I. H., and Turhan Çoban, M., "Thermal Conductivity of Particle Filled Polyethylene Composite Materials," *Composites Science and Technology*, Vol. 63, No. 1, 2003, pp. 113–117.

[12] Boudenne, A., Ibos, L., Fois, M., Gehin, E., and Majeste, J. C., "Thermophysical Properties of Polypropylene/Aluminium Composites," *Journal of Polymer Science Part B: Polymer Physics*, Vol. 42, No. 4, 2004, pp. 722–732.

[13] Tavman, I. H., "Effective Thermal Conductivity of Isotropic Polymer Composites," *International Communications in Heat and Mass Transfer*, Vol. 25, No. 5, 1998, pp. 723–732.

[14] Chung, D. D. L., "Materials for Thermal Conduction," *Applied Thermal Engineering*, Vol. 21, No. 16, 2001, pp. 1593–1605.

[15] Maxwell, J. C., *A Treatise on Electricity and Magnetism*, 3rd ed., Dover, New York, 1954, Chap. 9.

[16] Nielsen, L. E., "Thermal Conductivity of Particulate-filled Polymers," *Journal of Applied Polymer Science*, Vol. 17, No. 12, 1973, pp. 3819–3820.

[17] Nielsen, L. E., "The Thermal and Electrical Conductivity of Two-phase Systems," *Industrial & Engineering Chemistry Fundamentals*, Vol. 13, No. 1, 1974, p. 17.

[18] Agari, Y., Tanaka, M., Nagai, S., and Uno, T., "Thermal Conductivity of a Polymer Composite Filled With Mixtures of Particles," *Journal of Applied Polymer Science*, Vol. 34, No. 4, 1987, pp. 1429–1437.

[19] Agari, Y., Ueda, A., and Nagai, S., "Thermal Conductivity of a Polymer Composite," *Journal of Applied Polymer Science*, Vol. 49, No. 9, 1993, pp. 1625–1634.

[20] Agari, Y., Ueda, A., and Nagai, S., "Measurement of Thermal Diffusivity and Specific Heat Capacity of Polymers by Laser Flash Method," *Journal of Polymer Science Part B: Polymer Physics*, Vol. 33, No. 1, 1995, pp. 33–42.

[21] Feller, J. F., Linossier, I., Pimbert, S., and Levesque, G., "Carbon Black Filled Poly(ethylene-co-acrylates) Composites: Calorimetric Studies," *Journal of Applied Polymer Science*, Vol. 79, No. 5, 2001, pp. 779–793.

[22] Zienkiewicz, O. C., and Taylor, R. L., *Finite Element Method*, Vol. 1, 5th ed., Butterworth–Heinemann, Oxford, MA, 2000.

[23] FEMLAB User's Guide, ver. 2–3, COMSOL, Stockholm, Jan. 2003.

[24] Necati Özisik, M., *Heat Transfer, A Basic Approach*, McGraw–Hill, New York, 1985, Chaps. 1–3, p. 12.

[25] Feller, J. F., Chauvelon, P., Linossier, I., and Glouannec, P., "Characterization of Electrical and Thermal Properties of Extruded Tapes of Thermoplastic Conductive Polymer Composites (CPC)," *Polymer Testing*, Vol. 22, No. 7, 2003, pp. 831–837.